

---

# MOrdReD: Memory-based Ordinal Regression Deep Neural Networks for Time Series Forecasting

---

**Bernardo Pérez Orozco**  
University of Oxford  
Oxford, UK

**Gabriele Abbati**  
University of Oxford  
Oxford, UK

**Stephen Roberts**  
University of Oxford  
Oxford, UK

## Abstract

Time series forecasting is ubiquitous in the modern world. Applications range from health care to astronomy, include climate modelling, financial trading and monitoring of critical engineering equipment. To offer value over this range of activities we must have models that not only provide accurate forecasts but that also quantify and adjust their uncertainty over time. Furthermore, such models must allow for multimodal, non-Gaussian behaviour that arises regularly in applied settings. In this work, we propose a novel, end-to-end deep learning method for time series forecasting. Crucially, our model allows the principled assessment of predictive uncertainty as well as providing rich information regarding multiple modes of future data values. Our approach not only provides an excellent predictive forecast, shadowing true future values, but also allows us to infer valuable information, such as the predictive distribution of the occurrence of critical events of interest, accurately and reliably even over long time horizons. We find the method outperforms other state-of-the-art algorithms, such as Gaussian Processes.

only be related to the magnitude of the time series at an instant, but also to the timing of events of interest in it. Estimating timing uncertainty is thus a key challenge that has to be solved by accurately quantifying and propagating predictive uncertainty across a sequence of forecasts. Without this, models might either provide unrealistic bounds for their predictions in the long-term, or else revert back to their mean relatively quickly.

In the main, time series forecasting has been dominated by statistical models, often parametric (such as the family of Markovian and state-space models) and more recently by non-parametric approaches such as Gaussian Processes (GPs) (Rasmussen and Williams, 2006). These models however suffer from a number of shortcomings. For instance, poor scalability can hinder the use of the large amounts of data readily available in some tasks. Furthermore, assuming the predictive likelihood to be Gaussian, or an otherwise simple parametric distribution, could potentially be one additional restriction. Lastly, expert craftsmanship for model specification may also be required to attain best performance.

In parallel with parts of the latter developments, Recurrent Neural Networks (RNNs), and especially the Long Short Term Memory (LSTM) (Hochreiter and Schmidhuber, 1997), have shown themselves to offer excellent, end-to-end performance in predictions over symbol sequences, especially in the Natural Language Processing literature (Graves, Mohamed, and Hinton, 2013; Sutskever, Vinyals, and Le, 2014; Xu et al., 2014). LSTMs are able to efficiently propagate error signals back in time, which in turn enables them to quantify future outcomes over longer periods than alternative methods, such as GPs or random forests (Breiman, 2001). LSTMs therefore readily arise as suitable candidates to perform time series forecasting in a scalable and end-to-end fashion, while also allowing for principled computation of uncertainty bounds, as shown in recent work in the Bayesian Neural Network literature (Gal and Ghahramani, 2016b; Gal and Ghahramani, 2016a).

## 1 INTRODUCTION

Machine learning has a rich history over a wide range of time series forecasting tasks; recent examples include financial market predictions (Rutkauskas, Maknickas, and Maknickienė, 2011), energy output forecasting (Monteiro et al., 2013) and speech synthesis (Oord et al., 2016). In this setting, decision-makers rely on accurate predictions and reliable uncertainty bounds that enable them to make conclusions. Such uncertainty might not

In this work, we propose a novel approach in which the original time series forecasting problem is reformulated as an ordinal regression task. Most importantly, our approach is fully end-to-end as it does not require any expert model design intervention, nor makes explicit assumptions about the predictive distribution of the time series observations. Instead, our framework allows for direct learning from data in a nonparametric fashion. Furthermore, our model’s forecasts are accompanied by reliable and principled uncertainty bounds, as given in Gal and Ghahramani (2016b) and Gal and Ghahramani (2016a).

The contributions of our work can be listed as follows:

- We develop a fully end-to-end framework for long-term time series forecasting that requires little to no manual model tuning and outperforms other state-of-the-art techniques;
- we incorporate a sequential procedure to infer reliable long-term uncertainty bounds in an autoregressive fashion;
- we demonstrate how our probabilistic forecasts can be employed to predict the occurrence of critical events in a timely and reliable fashion.

The paper is organised as follows: in Section 2 we offer a review of existing approaches; in Section 3 we present an overview of the methods; in Section 4 the experiments that support the paper are detailed and we present our conclusions in Section 5.

## 2 RELATED WORK

Time series forecasting literature has a long history and covers a broad range of methods, including random forest regressors (Breiman, 2001), quantile random forests (Meinshausen, 2006) and more classic linear Markov models such as auto-regressive Moving Average (ARMA) methods. However, many methods (save for the linear Markov models, which can be recast as Bayesian linear models) fail to offer principled uncertainty quantification associated with the forecast.

In part, no doubt due to their native ability to infer full predictive distributions, Gaussian Process (Rasmussen and Williams, 2006) models have increasingly dominated the time series modelling literature over the last decade, especially as the classic Markov models (including AR processes and the like) can be seen as special cases of the GP. We simply note that, powerful though the GP approach is, the standard model makes the tacit assumption that the residuals are normally distributed and

hence the conditional predictive posterior is also a Gaussian.

Until recently, the literature on time series forecasting with neural networks, particularly recurrent neural nets, had been relatively scarce. A potential reason is that early findings showed that they were easily outperformed by simpler, memory-less methods (Gers, Eck, and Schmidhuber, 2001). Further, the methods were unable natively to provide reliable confidence intervals. Recently, however, the rise in the use of dropout (Gal and Ghahramani, 2016b; Gal and Ghahramani, 2016a) has enabled deep nets and recurrent models, including LSTMs, to provide principled confidence bounds. Indeed, recent work looks to apply these approaches to time series forecasting (Zhu and Laptev, 2017). This work, however, still makes the tacit assumption that the predictive distribution is unimodal Gaussian.

## 3 METHODS

In this section, we introduce our ordinal regression framework, which predicts time series in an ordinal fashion using a memory-endowed deep neural network (namely, an LSTM). We call this MOrdReD<sup>1</sup> (Memory-based Ordinal Regression Deep neural network).

We start by setting out what an ordinal regression task is in section 3.1. Then in section 3.2 we describe the LSTM, which forms the core of our forecasting. Finally, in section 3.3, we overview the link between dropout and Bayesian Neural Networks. The latter enables our model to handle uncertain (ordinal) observations, and thus achieve longer-term predictions with appropriate posterior distributions.

### 3.1 ORDINAL REGRESSION

Consider a bounded time series with range  $I \subset \mathbb{R}$  and let  $C = \{C_i\}_{i=1}^M$  be a partition of  $I$  with cardinality  $M$ . Without loss of generality, we assume the  $C_i$  have all the same measure on  $\mathbb{R}$  (e.g. the  $C_i$  are non-overlapping sub-intervals of  $I$  with equal sizes). Let  $\mathbf{x} = (\mathbf{x}_1, \dots, \mathbf{x}_T)$ , with  $\mathbf{x}_t \in \mathbb{R}^M$ , be the one-hot encoded representation of the time series after quantizing it over  $C$ .

We can then define the time series forecasting problem in an ordinal and auto-regressive fashion. Assume a sequence  $\mathbf{X}^{(i)} = (\mathbf{x}_1^{(i)}, \dots, \mathbf{x}_P^{(i)}) = (\mathbf{x}_{i-P+1}, \dots, \mathbf{x}_i)$ , where  $P$  is the lookback window horizon, is observed. The task of ordinal regression, which lies between regression and classification, consists in relating the latter sequence with a symbol  $\mathbf{y}^{(i)} \in C$ . It is straight-

<sup>1</sup>In Arthurian legend, Mordred was the illegitimate son of King Arthur. Mordred fell in battle with his own father.

forward to see that for the framework to work we need  $\mathbf{y}^{(i)} = \mathbf{x}_{P+1}^{(i)} = \mathbf{x}_{i+1}$ .

At this point it is useful to recap the notation used in this paper:

- $\mathbf{x}$ : quantized one-hot encoded representation of the continuous-assumed time series, with  $\mathbf{x}_i \in \mathbb{R}^M$ ;
- $\mathbf{X}$ :  $P$ -sample-long sub-sequence extracted from  $\mathbf{x}$ , this will represent an actual data point. Analogously as before, each element of  $\mathbf{X}$  is a vector lying in  $\mathbb{R}^M$ . Thus  $\mathbf{X} \in \mathbb{R}^{P \times M}$ .

Given  $M$  and  $P$ , the training datasets can be now defined as  $\mathcal{X} = \{\mathbf{X}^{(P)}, \dots, \mathbf{X}^{(N)}\}$  and  $\mathcal{Y} = \{\mathbf{y}^{(P)}, \dots, \mathbf{y}^{(N)}\}$ .

Nevertheless, it is true that such auto-regression comes with a potential loss of accuracy during the quantization phase. This can be mitigated by choosing a relatively large  $M$  that allows for a sufficiently coarse-grained partition  $C$ . LSTMs (introduced in the next section) thence naturally arise as a befitting methodology, due to their empirically proven ability to model categorical sequences over large numbers of symbols, such as those that frequently arise in the Natural Language Processing domain (Sutskever, Vinyals, and Le, 2014).

### 3.2 FORECASTING WITH LSTMS

In this section our forecasting method is introduced. We consider a Neural Network parameterized by a vector of parameters  $\theta$ , whose output is  $f^\theta(\mathbf{X})$ . In particular, we consider LSTM-based architectures trained on a dataset  $\mathcal{X}, \mathcal{Y}$ , with model likelihood  $p(\mathbf{y} | \mathbf{X}, \theta)$ .

#### 3.2.1 The Long Short Term Memory

The Long Short-Term Memory (LSTM) (Hochreiter and Schmidhuber, 1997) is a particular type of recurrent neural network (RNN) endowed with a gating mechanism that enables efficient propagation of error signals in time. Such mechanisms prevent well-known gradient instability issues that arise in other simple recurrent neural network models (Pascanu, Mikolov, and Bengio, 2013). Gating thus allows for efficient gradient-based learning of temporal features, which are encoded internally in memory cells that are updated with every new observation in the sequence.

Consider an observed sequence  $\mathbf{X} = (\mathbf{x}_1, \dots, \mathbf{x}_P)$ . For each  $t = 1, \dots, P$ , the LSTM outputs a vector of temporal features  $\mathbf{h}_t$ , which is given by

$$\mathbf{h}_t = \mathbf{o}_t \odot \tanh(\mathbf{C}_t). \quad (1)$$

$\mathbf{C}_t$  is the memory cell at time  $t$ :

$$\mathbf{C}_t = \mathbf{i}_t \odot \mathbf{S}_t + \mathbf{f}_t \odot \mathbf{C}_{t-1}, \quad (2)$$

where

$$\mathbf{S}_t = \tanh(\mathbf{W}_S \mathbf{x}'_t + \mathbf{b}_S) \quad (3)$$

and  $\mathbf{i}_t, \mathbf{o}_t, \mathbf{f}_t$  are the input, output and forget gates respectively:

$$\mathbf{i}_t = \sigma(\mathbf{W}_i \mathbf{x}'_t + \mathbf{b}_i), \quad (4)$$

$$\mathbf{o}_t = \sigma(\mathbf{W}_o \mathbf{x}'_t + \mathbf{b}_o), \quad (5)$$

$$\mathbf{f}_t = \sigma(\mathbf{W}_f \mathbf{x}'_t + \mathbf{b}_f). \quad (6)$$

Here  $\sigma$  is the sigmoid function,  $\odot$  is the element-wise product operator, and  $\mathbf{x}'_t = (\mathbf{x}_t, \mathbf{h}_{t-1})$  is the concatenation of the observation  $\mathbf{x}_t$  and the LSTM output at the previous timestep  $\mathbf{h}_{t-1}$ . Hence the learnable parameters of an LSTM are  $\theta = \{\mathbf{W}_i, \mathbf{W}_o, \mathbf{W}_f, \mathbf{W}_S, \mathbf{b}_i, \mathbf{b}_o, \mathbf{b}_f, \mathbf{b}_S\}$ .

#### 3.2.2 Sequence-to-Sequence

LSTMs can be further enriched by incorporating learnt features from the backwards temporal dynamics of the time series, in a bi-directional fashion. This model has shown remarkable success in the NLP literature (Graves and Schmidhuber, 2005), including extensions to LSTM-based models such as the sequence-to-sequence architecture (Sutskever, Vinyals, and Le, 2014). We now focus our attention to the latter. This particular model consists of two recurrent neural network models: an encoder  $f^{(\text{enc})}$ , which maps the observed sequence,  $\mathbf{X}$ , into a fixed-dimensional summary,  $\mathbf{h}_0^{(\text{dec})}, \mathbf{C}_0^{(\text{dec})}$ ; and a decoder  $f^{(\text{dec})}$ , which uses  $\mathbf{h}_0^{(\text{dec})}, \mathbf{C}_0^{(\text{dec})}$  as an informed initial state to predict future observations iteratively. More precisely:

$$\mathbf{h}_0^{(\text{dec})}, \mathbf{C}_0^{(\text{dec})} = f^{(\text{enc})}(\mathbf{X}), \quad (7)$$

$$\hat{\mathbf{y}}_t = \text{Softmax} \left( f^{(\text{dec})}(\mathbf{h}_{t-1}^{(\text{dec})}, \mathbf{C}_{t-1}^{(\text{dec})}, \mathbf{x}_t) \right) \quad (8)$$

#### 3.2.3 MOrdReD: an Ordinal Regression Sequence-to-Sequence framework

In our ordinal (auto-)regression setting, a sequence-to-sequence's encoder firstly produces a summary  $\mathbf{h}_0^{(\text{dec})}, \mathbf{C}_0^{(\text{dec})}$  of the last  $P$  observed samples of a one-hot encoded, quantized time series,  $\mathbf{X}^{(\text{enc})} = (\mathbf{x}_1, \dots, \mathbf{x}_P)$ . Then, the informed summary  $\mathbf{h}_0^{(\text{dec})}, \mathbf{C}_0^{(\text{dec})}$  is fed into the model's decoder, which observes the last available sample  $\mathbf{x}_P$  and finally outputs a class probability density  $\hat{\mathbf{y}}_P \in \mathbb{R}^M$  over the bins  $C$ , with  $\mathbf{x}_{P+1} \sim \hat{\mathbf{y}}_P$ .

It is now worth mentioning that  $\hat{\mathbf{y}}_P$  has two possible interpretations: on one hand, it is the categorical distribution that governs the behaviour of  $\mathbf{x}_{P+1}$ ; on the other

hand,  $\hat{\mathbf{y}}_P$  itself can be interpreted as a corrupted or otherwise noisy representation of  $\mathbf{x}_{P+1}$ . In our model, we enable direct autoregression by feeding back  $\hat{\mathbf{y}}_P$  into the decoder to forecast  $\mathbf{x}_{P+2} \sim \hat{\mathbf{y}}_{P+1}$ . We have observed empirically that such autoregression allows our model to perform better than by one-hot encoding either a statistic or a sample drawn from  $\hat{\mathbf{y}}_P$ . We argue that this is the case because the model has full information about its own previous decisions, including partial bin allocations.

This loopback process can be repeated an arbitrary number of times to forecast for long horizons, as we show in Section 4. During training time, we enable teacher forcing by allowing the decoder to see the true, uncorrupted observation  $\mathbf{X}_{P+k}$ ,  $k > 1$ . In other words, we jointly train the encoder and the decoder by allowing them to see  $\mathbf{X}^{(i)}$ ,  $\mathbf{X}^{(i+1)}$  respectively. At testing time however, the decoder only has access to at most 1 observed sample, which it uses as a seed to perform autoregression.

### 3.3 MC DROPOUT

In many tasks based on time series forecasting a single point estimate is not enough: uncertainty quantification and confidence bounds are often necessary tools for decision-making. Recent developments in the Bayesian Deep Learning literature have shown how a classic technique such as dropout can be interpreted as a Bayesian method and used to model uncertainty in neural networks.

#### 3.3.1 Classic Dropout

Dropout (Srivastava et al., 2014) is a stochastic regularization technique that has been successfully employed to prevent over-fitting and approximately combine different network architectures.

At training time, before each feed-forward operation (necessary to compute the gradients of the loss function), each connection of the neural network is dropped with probability  $p_{\text{drop}}$ . In this way, a mask computed according to this Bernoulli distribution is placed on the network, which in turn gets “thinned”. The gradients are computed, the weights are corrected and the process is repeated, this time with a different mask.

With this approach, a neural network with  $n$  units can be seen as a collection  $2^n$  thinned networks sharing a substantial number of weights. Furthermore, it has been found empirically that dropout leads to lower regularization errors than other regularization techniques.

#### 3.3.2 MC Dropout: the Bayesian Perspective

Coupled with a Monte Carlo approach, dropout can be used to model uncertainty in classic neural networks (Gal and Ghahramani, 2016b). This derives from the fact that, under certain assumptions, a neural network of arbitrary depth trained with dropout before each layer is mathematically equivalent to a probabilistic Gaussian Process (Damianou and Lawrence, 2013).

With these premises, the predictive distribution of the model presented in section 3.2.3 is:

$$p(\mathbf{y}^*|\mathbf{X}^*) = \int p(\mathbf{y}^*|\mathbf{X}^*, \boldsymbol{\theta})p(\boldsymbol{\theta})d\boldsymbol{\theta}, \quad (9)$$

where  $p(\boldsymbol{\theta})$  denotes the dropout (Bernoulli) distribution acting as described in section 3.3.1. It is then possible to approximate the integral via Monte Carlo:

$$p(\mathbf{y}^*|\mathbf{X}^*) \approx \frac{1}{N_s} \sum_{n=1}^{N_s} \text{Softmax} \left( f^{\hat{\boldsymbol{\theta}}^{(n)}}(\mathbf{X}^*) \right), \quad (10)$$

where  $\hat{\boldsymbol{\theta}}^{(n)} \sim p(\boldsymbol{\theta})$ .

Thanks to the theoretical results that connect Deep Gaussian Processes with neural networks, the use of the above mean for the predictive distribution is grounded and justified.

So far, we have not specified any characteristic of the neural network we are applying the dropout scheme to. In Gal and Ghahramani (2016a) the authors make a theoretically-sound argument for the application of dropout to recurrent neural networks. In essence, the masks need to be fixed for all the recursive passes. This is the approach we follow when performing the experiments illustrated in the next Section.

### 3.4 REMARKS

Two crucial aspects to highlight about our framework are the following. Firstly, we achieve end-to-end time series forecasting by allowing our model to learn directly from data. Importantly, we do not make use of handcrafted features, nor require expert knowledge to specify parts of the model (as often required in GPs for instance).

Secondly, our model learns a non-parametric predictive posterior at each time step. This allows for rich, multimodal behaviour to be encoded and fed back in an autoregressive fashion. We have observed empirically that providing our model with full knowledge of its own previous decisions enables it to achieve more reliable, longer-term forecasting than by one-hot encoding some statistic (such as the empirical mean or the mode) at every timestep.

## 4 EXPERIMENTS

In this section, we display our model’s performance in two different uncertainty quantification tasks. Our datasets and baselines are introduced in sections 4.1 and 4.2. Then, in sections 4.3.1 and 4.4.1, we benchmark our model in the settings of long-term uncertainty quantification and event occurrence forecasting.

### 4.1 DATASETS

We chose three different quasi-periodic time series with 10,000 to 20,000 samples each to showcase the performance of the models in different application fields:

- **Mackey-Glass chaotic attractor**, to highlight prediction on chaotic data;
- a recording of the **electrical activity of the human heart**, to highlight forecasting of a quasi-periodic, complex-shaped signal where accurate timing is essential;
- data taken from **environmental sensors** that record tide heights in an off-shore weather station.

All three datasets are quantized into  $M$  bins. Within reason, the choice of  $M$  (problem dependent and a trade-off between resolution and computational simplicity) does not affect results. In our work, we used the following heuristic: for a bounded time series  $\mathbf{x}$ , consider  $\dot{\mathbf{x}} = (\dot{\mathbf{x}}_1, \dots, \dot{\mathbf{x}}_{N-1})$  obtained by computing its first-order finite differences, and  $p(\dot{x})$ , the empirical distribution over its values. For some proportion  $0 < \alpha < 1$ , consider the the quantile  $q_\alpha$  of  $p(\dot{x})$ . Then, choose

$$M = \left\lceil \frac{1}{q_\alpha} \right\rceil. \quad (11)$$

Following this heuristic,  $M$  is chosen reciprocal to the rate of change  $q_\alpha$  that guarantees that a proportion  $\alpha$  of contiguous samples will still be allocated to different bins during quantisation. In our work, we used  $\alpha = 0.95$ , though we do not observe extreme sensitivity to this choice.

### 4.2 BASELINE MODEL

We compare our framework against another state-of-the-art model, the Gaussian Process, which we review briefly below.

#### 4.2.1 Gaussian Processes

Gaussian processes describe distributions over functions. They are defined as a collection of random variables,

any finite number of which have a joint Gaussian distribution. A GP  $f$  is fully specified by a mean function  $m(\mathbf{x}) = \mathbb{E}[f(\mathbf{x})]$  and a covariance function  $k(\mathbf{x}, \mathbf{x}') = \mathbb{E}[(f(\mathbf{x}) - m(\mathbf{x}))(f(\mathbf{x}') - m(\mathbf{x}'))]$ . The covariance function (or kernel) describes correlations between data points and can be used to encapsulate prior belief about the problem. We refer the reader to Rasmussen and Williams (2006) for a more detailed discussion about Gaussian Processes.

Consider a time series of length  $N$ . Long-term forecasting with GPs can be achieved in two different ways:

- **Univariate temporal GP**. The Gaussian Process  $f$  is used to directly model the time series as a function of time.
- **Autoregressive GP (ARGP)**. The Gaussian Process  $f$  is trained to map a sequence of length  $P$   $\mathbf{X} = (\mathbf{x}_{N-P+1}, \dots, \mathbf{x}_N)$  to a normal distribution over its next sample  $\mathcal{N}(\mathbf{x}_{N+1} \mid \boldsymbol{\mu}_{N+1}, \boldsymbol{\sigma}_{N+1}^2)$ . In an autoregressive fashion, the forecast at time  $N+1$  is used to compute the one at time  $N+2$  and so on. However, uncertainty estimates for following predictions require to adequately forward-propagate the uncertainty computed in previous forecasts. This is discussed below in more detail.

#### 4.2.2 Propagating uncertainty in autoregressive GPs

Uncertain, or noisy input, GPs are analytically intractable and therefore developing approximations remains an active area of research. In our work, we use an Monte Carlo-based approach (Girard and Murray-Smith, 2005).  $S_{\text{GP}}$  sample trajectories are drawn up to time  $N + P_h$  for a predictive horizon  $P_h$ , i.e.  $\hat{\mathbf{X}}^{[s]} = (\hat{\mathbf{x}}_{N+1}^{[s]}, \dots, \hat{\mathbf{x}}_{N+P_h}^{[s]})$ , and used to estimate the moments  $\tilde{\boldsymbol{\mu}}_{N+k}, \tilde{\boldsymbol{\sigma}}_{N+k}^2$  of the corrected normal distribution  $p(\mathbf{x}_{N+k} \mid \tilde{\boldsymbol{\mu}}_{N+k}, \tilde{\boldsymbol{\sigma}}_{N+k}^2)$ .

Each sample trajectory is built iteratively  $\forall k, 2 \leq k \leq P_h$  in the following fashion:

1. at time  $N + k - 1$ , compute  $\mathcal{N}(\mathbf{x}_{N+k-1} \mid \boldsymbol{\mu}_{N+k-1}, \boldsymbol{\sigma}_{N+k-1}^2)$  from the sequence  $\hat{\mathbf{X}}^{(N+k-2)}$ ,
2. draw a sample  $\hat{\mathbf{x}}_{N+k-1}^{[s]}$  from  $\mathcal{N}(\mathbf{x}_{N+k-1} \mid \boldsymbol{\mu}_{N+k-1}, \boldsymbol{\sigma}_{N+k-1}^2)$ , and build the next input seed sequence  $\hat{\mathbf{X}}^{(N+k-1)} = (\mathbf{x}_{N+k-P+1}, \dots, \mathbf{x}_{N+k-1})$ ,
3. repeat from step 1 until  $k > P_h$ .

After repeating the procedure above  $S_{\text{GP}}$  times, the corrected mean and variance  $\forall k, 2 \leq k \leq P_h$  are thence

given by:

$$\tilde{\mu}_{N+k} = \mathbb{E}[\mathbf{x}_{N+k}] \approx \frac{1}{S_{\text{GP}}} \sum_{s=1}^{S_{\text{GP}}} \hat{\mathbf{x}}_{N+k}^{[s]} \quad (12)$$

$$\begin{aligned} \tilde{\sigma}_{N+k}^2 &= \mathbb{E}[(\mathbf{x}_{N+k})^2] - \mathbb{E}[\mathbf{x}_{N+k}]^2 \quad (13) \\ &\approx \frac{1}{S_{\text{GP}}} \sum_{s=1}^{S_{\text{GP}}} \left( \hat{\mathbf{x}}_{N+k}^{[s]} - \tilde{\mu}_{N+k} \right)^2 \end{aligned}$$

### 4.3 QUANTIFYING LONG-TERM UNCERTAINTY

#### 4.3.1 Experimental setup

In this experiment, we benchmark our MOrdReD architecture against both, univariate and autoregressive GPs, to quantify uncertainty in long-term forecasting. We remark that other baselines, namely Quantile Random Forests and AR( $p$ ) models were also trained. However, they both underperformed with respect to our GP baselines in both predictive accuracy and uncertainty bound estimation (in the case of Quantile Forests). In the case of Quantile Forests, their forecasts grew overconfident and out of phase with the ground true in the long term; in the case of AR( $p$ ), the prediction reverted back the mean after relatively few samples. This is why we opted for a more detailed comparison between GPs and our framework.

Our long-term forecasting task consists in extrapolating  $P_h$  emissions ( $\hat{\mathbf{x}}_{N+1}, \dots, \hat{\mathbf{x}}_{N+P_h}$ ) forward from the last  $P$  observations ( $\mathbf{x}_{N-P}, \dots, \mathbf{x}_N$ ) in the time series of length  $N$ , with  $P \ll P_h$ . In our setting, we chose  $P = 100, P_h = 1000$ .

Crucially, the goal in this experiment is not to evaluate a model's predictive accuracy, but rather its honesty expressed through their uncertainty estimations. That is, we prefer models that are able to either produce an accurate confident forecast, or otherwise explicitly confess their ignorance - for instance, through a mean-reversal process.

We quantify this via the negative sequence log-likelihood, which we rewrite using the chain rule for joint distributions:

$$\begin{aligned} -\log p(\mathbf{X}^{(N+P_h)}) &= -\log p(\mathbf{x}_{N+1}) \quad (14) \\ &- \sum_{k=2}^{P_h} \log p\left(\mathbf{x}_{N+k} \left| \bigcap_{k'=1}^{k-1} \mathbf{x}_{N+k'} \right.\right) \end{aligned}$$

#### 4.3.2 Computing the negative sequence log-likelihood

In the case of the univariate GP, the negative log-likelihood of the prediction  $\mathbf{X}^{(N+P_h)}$  is

$$\text{NLL}_{\text{GP}}(\mathbf{X}^{(N+P_h)}) = - \sum_{k=1}^{P_h} \log \mathcal{N}(\mathbf{x}_{N+k} \mid \boldsymbol{\mu}_{N+k}, \boldsymbol{\sigma}_{N+k}^2) \quad (15)$$

For the autoregressive GP, the factor  $p(\mathbf{x}_{N+k} \mid \bigcap_{k'=1}^{k-1} \mathbf{x}_{N+k'})$  is approximated using the adjusted parameters  $\tilde{\mu}_{N+k}, \tilde{\sigma}_{N+k}^2$ :

$$\begin{aligned} \text{NLL}_{\text{ARGP}} \approx & - \log \mathcal{N}(\mathbf{x}_{N+1} \mid \boldsymbol{\mu}_{N+1}, \boldsymbol{\sigma}_{N+1}^2) \quad (16) \\ & - \sum_{k=2}^{P_h} \log \mathcal{N}(\mathbf{x}_{N+k} \mid \tilde{\boldsymbol{\mu}}_{N+k}, \tilde{\boldsymbol{\sigma}}_{N+k}^2) \end{aligned}$$

Finally, we describe how to compute the negative sequence log-likelihood for our MOrdReD model. Consider the categorical output  $\hat{\mathbf{y}}_t$  over the partition  $C$  of intervals  $C_i$ , each of length  $|C_i|$ . Then we can straightforwardly construct a stepwise uniform probability density function over the range of the time series  $I$ :

$$\begin{aligned} p(\mathbf{x}_{t+1} \mid \mathbf{x}_t, \dots, \mathbf{x}_{t-P+1}) &= p_{\text{MOR}}(\mathbf{x}_{t+1} \mid \hat{\mathbf{y}}_t) \quad (17) \\ &= \prod_{i=1}^M \frac{\hat{\mathbf{y}}_t(i)^{\mathbb{I}[\mathbf{x}_{t+1} \in C_i]}}{|C_i|} \end{aligned}$$

$$\begin{aligned} \log p_{\text{MOR}}(\mathbf{x}_{t+1} \mid \hat{\mathbf{y}}_t) &= \sum_{i=1}^M \pi_{t+1}^i \log \frac{\hat{\mathbf{y}}_t(i)}{|C_i|} \quad (18) \\ \pi_{t+1}^i &= \mathbb{I}[\mathbf{x}_{t+1} \in C_i] \end{aligned}$$

The negative sequence log-likelihood can now be calculated as:

$$\begin{aligned} \text{NLL}_{\text{MOR}} &= -\log \prod_{k=1}^{P_h} \prod_{i=1}^M \frac{\hat{\mathbf{y}}_{N+k-1}(i)^{\pi_{N+k}^i}}{|C_i|} \quad (19) \\ &= -\sum_{k=1}^{P_h} \sum_{i=1}^M \pi_{N+k}^i \log \frac{\hat{\mathbf{y}}_{N+k-1}(i)}{|C_i|} \end{aligned}$$

#### 4.3.3 Model configuration

For our neural network models, we used Keras (Chollet, 2015) with the Tensorflow (Abadi et al., 2015) backend. We employed the Adam (Kingma and Ba, 2014) optimizer to minimize the categorical cross-entropy loss function between the one-hot encoded target vectors and the softmax output  $\hat{\mathbf{y}}$ . The network hyperparameters are defined over the hypergrid given by the hidden units  $h_u \in [32, 75, 150, 256, 384]$ , the dropout rate  $p_{\text{drop}} \in [0.2, 0.3, 0.5]$  and the L2 regularization constant  $\lambda \in [1e-5, \dots, 1e-10]$ .

Table 1: Models and configurations used in our experiments.

Model	Tide height
MOrdReD	$p_{(\text{drop})} = 0.2, \lambda = 1e - 10, h_u = 384$
UnivarGP	Quasiperiodic
ARGP	Matérn 5/2 + Bias
	Mackey-Glass
MOrdReD	$p_{(\text{drop})} = 0.2, \lambda = 1e - 8, h_u = 75$
UnivarGP	Matérn 5/2
ARGP	Matérn 5/2
	ECG
MOrdReD	$p_{(\text{drop})} = 0.5, \lambda = 1e - 9, h_u = 128$
UnivarGP	Quasiperiodic
ARGP	Matérn 5/2

For our Gaussian Process models, we used the open source library GPy (GPy, 2012). For both, univariate and autoregressive kernels, we validated across a number of kernels: Matérn 5/2, Quasiperiodic (Rational Quadratic  $\times$  Periodic), Radial Basis Function, Periodic Matérn 5/2. These were all tested out both with a bias and without. The final configurations for our models are given in Table 1.

#### 4.3.4 Results

Sequence negative log-likelihoods for each of our models are shown in Table 2. As observed, our ordinal regression framework outperforms our state-of-the-art baselines in two out of three datasets under this metric, and also achieves competitive performance in the remaining dataset. In Figures 1, 2 and 3, we compare the predictions given by the best-performing baseline (ARGP) and our MOrdReD framework. For the electrocardiogram dataset, all baselines reverted back to their mean relatively quickly in the task, which is why we only provide plots for the MOrdReD results for this dataset.

Our model achieves state-of-the-art performance in an end-to-end fashion, by learning structure directly from data. Unlike GP Regression, where knowledge of kernels is required and often inaccessible to unfamiliar users, our framework is end-to-end and only requires intervention to define the hyperparameter grid of hidden units, dropout rate and L2 regularization. Additionally, other advantages of neural networks such as scalability are now accessible. Our framework can make the most out of big datasets and produce reliable forecasts in the long term that outperform other state-of-the-art techniques.

As it can be seen in Figures 1, 2 and 3, error bars become wider over time. This allows models to speak about timing or phase uncertainty in the time series. In domains

Table 2: Negative sequence log-likelihood for 1000 out-of-sample forecasts from 100 observed samples. Figures in **bold** indicate best performance.

Model	Tide height	Mackey-Glass	ECG
MOrdReD	<b>1027.18</b>	824.34	<b>-101.98</b>
ARGP	1531.11	<b>715.86</b>	1710.37
UnivarGP	18557.18	1414.64	1446.68

such as health care and meteorology, forecasting *when* an event will happen could potentially be of more relevance than simply knowing its amplitude.

## 4.4 QUANTIFYING EVENT TIMING UNCERTAINTY

Consider the tide height dataset introduced in section 4.1. Experts are often interested in knowing *when* the tide levels will reach its maximum or minimum height. But despite it being a periodic phenomenon, sensor quantization leads to representation errors that make the time series quasiperiodic in practice.

In a similar vein, cardiologists are interested for instance in forecasting the timing of the QRS complex (characterised by the peaks observed in Figure 2). Predicting these timings further enables them to compute other metrics of interest, such as the RR interval – which has been linked, for instance, to Parkinson’s disease. Accurately quantifying these metrics is therefore of utmost importance, and fully relies on models that can speak honestly about their forecasts and their uncertainties.

In order to adequately quantify event timings, we construct a non-parametric probability distribution  $p(t)$  that describes the probability of an event happening at time  $t$ . We consider three such events in our experiment: the QRS complex in the electrocardiogram dataset, as well as the maxima and minima in the tide height one.

### 4.4.1 Experimental setup

The task in this experiment is to predict when a certain event will happen, alongside reliable uncertainty bounds. In this setting we compare our MOrdReD framework and our best-performing baseline, the autoregressive GP.

To compute such timing forecasts, we employ Kernel Density Estimation (KDE) to construct a probability density function  $p(t)$  that describes the probability that a certain event will happen at time  $t$ . KDE is a smoothing technique that builds a non-parametric distribution from

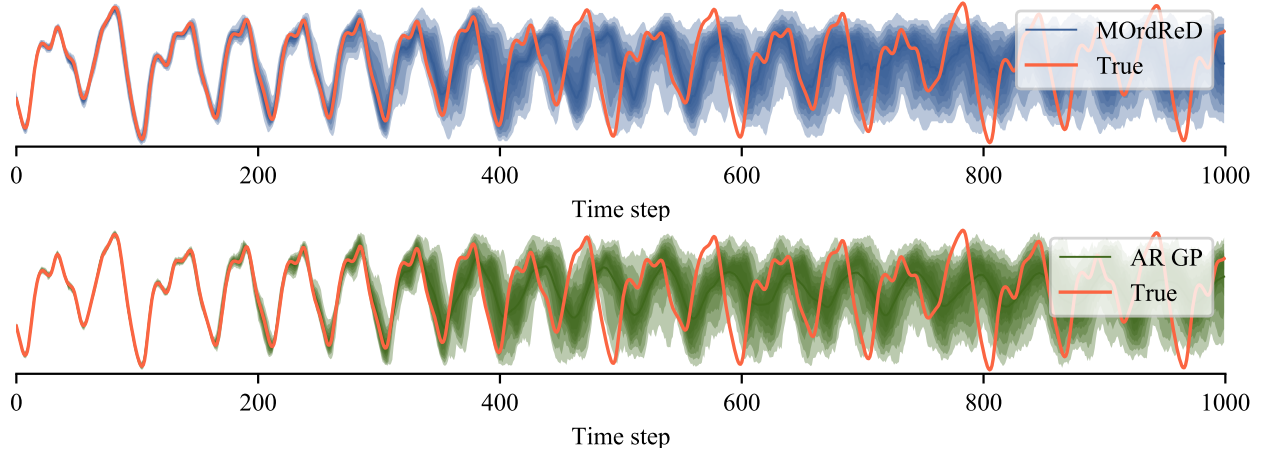


Figure 1: Out-of-sample Mackey-Glass forecasts with MOrdReD (top) and AR GP (bottom). Color shades describe the quantiles  $q_\alpha$  between  $q_{0.05}$  and  $q_{0.95}$  at each time step.

a sample set  $X$ . The estimator is given by

$$p(t) = \frac{1}{n} \sum_{i=1}^{|X|} K_h(t - t_i), \quad (20)$$

where  $t_i \in X$ ,  $K_h$  is a non-negative function that integrates to one, and  $h$  is the bandwidth hyperparameter. The reader is referred to Hastie, Tibshirani, and Friedman (2001) for a more detailed discussion. In our work, we used the freely available implementation of Scikit-learn (Pedregosa et al., 2011).

In the case of ARGPs, consider the forecast distributions described in section 4.3.1,  $\mathcal{N}(\mathbf{x}_{N+k} | \tilde{\boldsymbol{\mu}}_{N+k}, \tilde{\boldsymbol{\sigma}}_{N+k}^2), 2 \leq k \leq P_h$ .  $N_S$  sample trajectories are drawn as described in section 4.2.1, and the timing of the desired event in each sample is recorded. This yields a timing list  $X = (t_1, \dots, t_L)$  from which a density estimator can be built as described previously.

In our framework, a similar sampling scheme is proposed. This is achieved simply by running MOrdReD  $N_S$  times, each with a different dropout mask as described in section 3.3. The timings  $t_i$  of the desired event are then recorded for each sample forecast to construct a list  $X = (t_1, \dots, t_L)$  from which a density estimator can be built.

Now consider the true event timings  $X^{(\text{true})} = (t_1^{(\text{true})}, \dots, t_{L'}^{(\text{true})})$ . The constructed densities are then evaluated in terms of the negative log-likelihood for effectively predicting such correct timings:

$$\text{NLL}_{X^{\text{true}}} = -\log \prod_{i=1}^{L'} p(t_i^{(\text{true})}) = -\sum_{i=1}^{L'} \log p(t_i^{(\text{true})}) \quad (21)$$

Table 3: Negative log-likelihood for event detection. Figures in **bold** indicate best performance.

Model	Tide peaks	Tide minimum	ECG
MOrdReD	<b>35.71</b>	<b>34.64</b>	<b>-54.13</b>
ARGP	35.81	38.96	X

#### 4.4.2 Results

In Table 3 the negative log-likelihood values for drawing the true timings  $X^{(\text{true})}$  from the constructed densities  $p_{\text{ARGP}}(t), p_{\text{MOR}}(t)$  are shown for three different events: tide height maximum, tide height minimum, and QRS complex. As explained in section 4.3.4, the ARGP electrocardiogram results and plot are not provided due to its extremely poor performance in long term forecasting.

It can be seen that under this metric our model outperforms its competitor, especially in the case of the electrocardiogram as the best baseline is unable to produce a long-term forecast. Results can also be visualized more clearly in the upper subplots of Figures 2 and 3, which showcase the obtained densities for the occurrence of peak height and QRS complex in our tide height and electrocardiogram datasets.

## 5 CONCLUSIONS

In this article we have introduced a novel ordinal time series forecasting method based on recurrent neural networks. Our model is able empirically to outperform other state-of-the-art competitors in terms of long-term forecasting uncertainty estimation, while also inheriting all the advantages of neural network models.

Importantly, our framework is fully end-to-end and re-



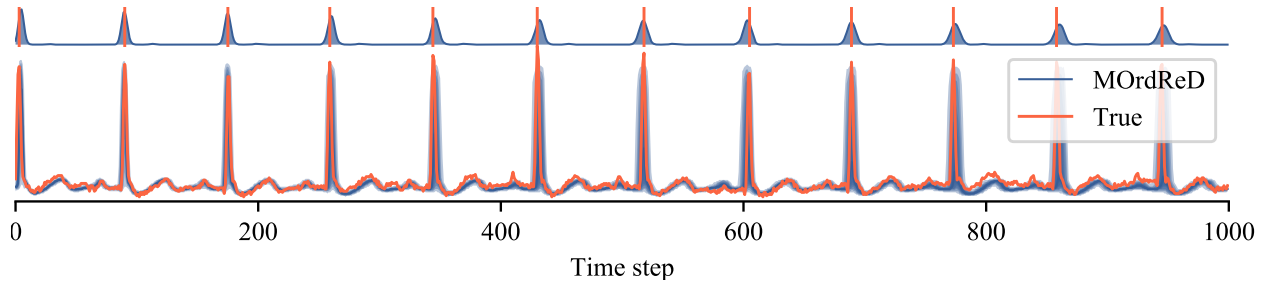


Figure 2: Out-of-sample electrocardiogram forecasts with MOrdReD. Color shades describe the quantiles  $q_\alpha$  between  $q_{0.05}$  and  $q_{0.95}$  at each time step. The upper subplot describes the probability that the QRS complex peak will occur at time  $t$ .

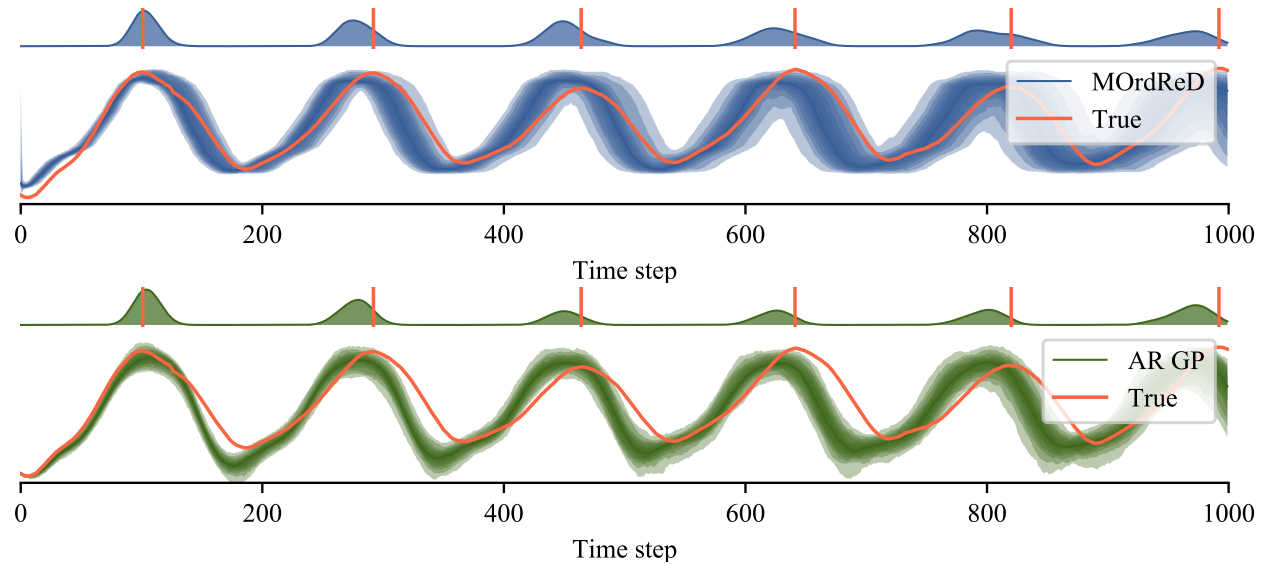


Figure 3: Out-of-sample tide height forecasts with MOrdReD (top) and AR GP (bottom). Color shades describe the quantiles  $q_\alpha$  between  $q_{0.05}$  and  $q_{0.95}$  at each time step. The upper subplot describes the probability that tide height will reach its peak at time  $t$ .

quires little intervention. Direct learning from data is thence enabled without compromising scalability, assuming Gaussian predictive distributions, or requiring extensive knowledge of available kernels (as is the case for models such as Gaussian Processes).

Finally, we showed how our model can be used to construct the predictive distribution of the occurrence of critical events of interest. We provided evidence that our framework yields long-term, reliable confidence intervals even in safety-critical environments such as cardiology and meteorology.

## References

- Abadi, Martín et al. (2015). *TensorFlow: Large-Scale Machine Learning on Heterogeneous Systems*. Software available from tensorflow.org. URL: <https://www.tensorflow.org/>.
- Breiman, Leo (2001). “Random forests”. In: *Machine learning* 45.1, pp. 5–32.
- Chollet, François (2015). *Keras*. <https://github.com/fchollet/keras>.
- Damianou, Andreas and Neil Lawrence (2013). “Deep gaussian processes”. In: *Artificial Intelligence and Statistics*, pp. 207–215.
- Gal, Yarin and Zoubin Ghahramani (2016a). “A theoretically grounded application of dropout in recurrent neural networks”. In: *Advances in neural information processing systems*, pp. 1019–1027.
- (2016b). “Dropout as a Bayesian Approximation: Representing Model Uncertainty in Deep Learning”. In: *Proceedings of The 33rd International Conference on Machine Learning*. Ed. by Maria Florina Balcan and Kilian Q. Weinberger. Vol. 48. Proceed-

- ings of Machine Learning Research. New York, New York, USA: PMLR, pp. 1050–1059. URL: <http://proceedings.mlr.press/v48/gall16.html>.
- Gers, Felix A, Douglas Eck, and Jürgen Schmidhuber (2001). “Applying LSTM to Time Series Predictable through Time-Window Approaches”. In: *Artificial Neural Networks — ICANN 2001: International Conference Vienna, Austria, August 21–25, 2001 Proceedings*. Ed. by Georg Dorffner, Horst Bischof, and Kurt Hornik. Berlin, Heidelberg: Springer Berlin Heidelberg, pp. 669–676. ISBN: 978-3-540-44668-2. DOI: 10.1007/3-540-44668-0\_93. URL: [http://dx.doi.org/10.1007/3-540-44668-0\\_{\\\_}93](http://dx.doi.org/10.1007/3-540-44668-0_{\_}93).
- Girard, Agathe and Roderick Murray-Smith (2005). “Gaussian processes: Prediction at a noisy input and application to iterative multiple-step ahead forecasting of time-series”. In: *Switching and Learning in Feedback Systems*. Springer, pp. 158–184.
- GPy (2012). *GPy: A Gaussian process framework in Python*. <http://github.com/SheffieldML/GPy>.
- Graves, A. and J. Schmidhuber (2005). “Framewise phoneme classification with bidirectional LSTM networks”. In: *Proceedings. 2005 IEEE International Joint Conference on Neural Networks, 2005*. Vol. 4, 2047–2052 vol. 4. DOI: 10.1109/IJCNN.2005.1556215.
- Graves, Alex, Abdel-rahman Mohamed, and Geoffrey Hinton (2013). “Speech Recognition With Deep Recurrent Neural Networks”. In: *ICASSP*. ISSN: 1520-6149. DOI: 10.1109/ICASSP.2013.6638947. arXiv: arXiv:1303.5778v1.
- Hastie, Trevor, Robert Tibshirani, and Jerome Friedman (2001). *The Elements of Statistical Learning*. Springer Series in Statistics. New York, NY, USA: Springer New York Inc.
- Hochreiter, Sepp and Jürgen Schmidhuber (1997). “Long short-term memory.” In: *Neural computation* 9.8, pp. 1735–80. ISSN: 0899-7667. DOI: 10.1162/neco.1997.9.8.1735. arXiv: 1206.2944. URL: <http://www.ncbi.nlm.nih.gov/pubmed/9377276>.
- Kingma, Diederik and Jimmy Ba (2014). “Adam: A Method for Stochastic Optimization”. In: *International Conference on Learning Representations*, pp. 1–13. arXiv: 1412.6980. URL: <http://arxiv.org/abs/1412.6980>.
- Meinshausen, Nicolai (2006). “Quantile regression forests”. In: *Journal of Machine Learning Research* 7. Jun, pp. 983–999.
- Monteiro, Claudio et al. (2013). “Short-Term Power Forecasting Model for Photovoltaic Plants Based on Historical Similarity”. In: *Energies — Open Access Energy Research, Engineering and Policy Journal*, pp. 2624–2643. DOI: 10.3390/en6052624.
- Oord, Aaron van den et al. (2016). “WaveNet: A Generative Model for Raw Audio”. In: *CoRR* abs/1609.03499. URL: <http://arxiv.org/abs/1609.03499>.
- Pascanu, Razvan, Tomas Mikolov, and Yoshua Bengio (2013). “On the difficulty of training recurrent neural networks”. In: *Proceedings of The 30th International Conference on Machine Learning* 28.2, pp. 1310–1318. ISSN: 1045-9227. DOI: 10.1109/72.279181. arXiv: arXiv:1211.5063v2. URL: <http://jmlr.org/proceedings/papers/v28/pascanu13.pdf>.
- Pedregosa, F. et al. (2011). “Scikit-learn: Machine Learning in Python”. In: *Journal of Machine Learning Research* 12, pp. 2825–2830.
- Rasmussen, Carl Edward and Christopher K. I. Williams (2006). *Gaussian Processes for Machine Learning*. The MIT Press.
- Rutkauskas, Aleksandras Vytautas, Algirdas Maknickas, and N Maknickienė (2011). “Investigation of financial market prediction by recurrent neural network”. In: *Innovative Infotechnologies for Science, Business and Education* 2.687, pp. 3–8.
- Srivastava, Nitish et al. (2014). “Dropout: A simple way to prevent neural networks from overfitting”. In: *The Journal of Machine Learning Research* 15.1, pp. 1929–1958.
- Sutskever, Ilya, Oriol Vinyals, and Quoc V. Le (2014). “Sequence to Sequence Learning with Neural Networks”. In: *Advances in Neural Information Processing Systems 27: Annual Conference on Neural Information Processing Systems 2014, December 8–13 2014, Montreal, Quebec, Canada*. Ed. by Zoubin Ghahramani et al., pp. 3104–3112. URL: <http://papers.nips.cc/paper/5346-sequence-to-sequence-learning-with-neural-networks>.
- Xu, Kelvin et al. (2014). “Show, Attend and Tell: Neural Image Caption Generation with Visual Attention”. In: *Proceedings of Machine Learning Research*. arXiv: arXiv:1502.03044v3.
- Zhu, Lingxue and Nikolay Laptev (2017). “Deep and Confident Prediction for Time Series at Uber”. In: *Data Mining Workshops (ICDMW), 2017 IEEE International Conference on*. IEEE, pp. 103–110.